Journal of Physics: Conference Series

PAPER • **OPEN ACCESS**

Study of the adsorption of dyes employed in the food industry by activated carbon based on residual forestry

To cite this article: C Valladares *et al* 2019 *J. Phys.: Conf. Ser.* **1173** 012009

Study of the adsorption of dyes employed in the food industry by activated carbon based on residual forestry

C Valladares[1], J F Cruz[2], L Matějová[3], E Herrera[1], M M Gómez[4], J L Solís[4], K Soukup[5], O Šolcová [5] and G J F Cruz [1]*

[1]Department of Forestry Engineering and Environmental Management, Universidad Nacional de Tumbes, Av. Universitaria s/n, Campus Universitario – Pampa Grande, Tumbes, Peru
[2]Department of Chemistry, Universidad Nacional de Piura, Campus Universitario – Miraflores s/n, Piura, Peru
[3]Institute of Environmental Technology, VŠB – Technical University of Ostrava, 17. Listopadu 15/2172, CZ-708 00 Ostrava-Poruba, Czech Republic
[4]Faculty of Sciences, Universidad Nacional de Ingeniería, Av. Túpac Amaru 210, Lima 25, Peru
[5]Institute of Chemical Process Fundamentals of the CAS, v. v. i, Rozvojová 135, Prague 6, Czech Republic

*E-mail: gcruzc@untumbes.edu.pe

Abstract. An activated carbon (adsorbent) was prepared from a forestry residual biomass (*Capparis scabrida* sawdust) by chemical activation with $ZnCl_2$. The adsorbent was tested in kinetic experiments to remove three anionic dyes widely used in the food industry: tartrazine (TR), brilliant scarlet 4R (BS4R) and brilliant blue (BB). The adsorbent was able to remove the dyes in different intensities, and the revealed order of their adsorption ability was BS4R>TR>BB. Most of the kinetic data fit best to the pseudo-second order model; however, high accordance with other models indicates that there is more than one phenomenon to explain the adsorption process. Analyzing the data that fit well to the pseudo-second order model and considering that the equilibrium was reached, the equilibrium adsorption capacity (q_e) for TR was 55.3 mg/g (when the AC load was 1 g/l and the TR initial concentration was 50 mg/l); for BS4R, 72.1 mg/g (when the AC load was 1 g/l and the TR initial concentration was 50 mg/l); and for BB, 14.1 mg/g (when the AC load was 1 g/l and the TR initial concentration was 10 mg/l) as the maximum values. AC based on *Capparis scabrida* residual biomass is a promising material for use in the purification of water polluted by anionic azo dyes.

1. Introduction

Dyes are widely used in different industries, such as textile [1], food [2] and cosmetic industries. Three of the dyes used extensively in the food industry are tartrazine (TR), brilliant scarlet 4R (BS4R) and brilliant blue (BB) (table 1 shows the chemical structure and some properties of the dyes). A portion of these dyes are disposed of (approximately 10%) in wastewater during production and consumption, even though they are toxic agents for aquatic species [3]. Although these dyes are dangerous for human health [4, 5], in most countries they are still permitted [6].

Table 1. Properties of the dyes used in this study.

Dye	Formula	Codes	Type	Molecular weight (g/mol)
Tartrazine [7]	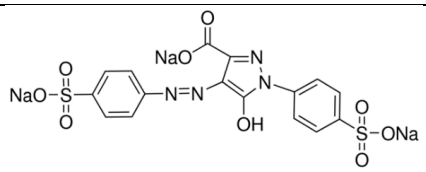	CI19140, E102	Anionic, Azo	534.3
Brilliant scarlet 4R [8, 9]	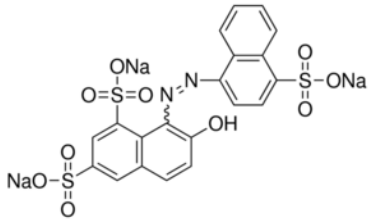	CI16255, E124	Anionic, Azo	604.46
Brilliant blue [10]	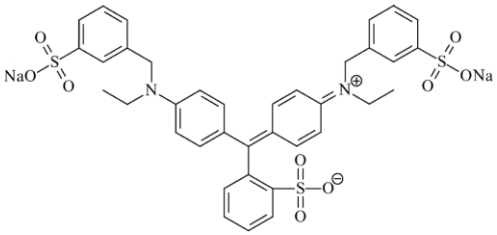	CI42090, E133	Anionic, Azo	792.85

Producing residual forestry biomass is very common in Peru. Currently, some low-cost materials are used to produce byproducts such as construction materials. However, there is another part of this residual biomass that is disposed of in areas without technical and environmental minimum acceptable conditions. In some cases, the residual biomass is burned in open field conditions, causing negative environmental impacts. *Capparis scabrida* is one of the species from dry forest in northwest Peru that is commonly used to produce handicrafts and cookware. Nevertheless, the residual biomass (sawdust mainly) from *Capparis scabrida* processing workshops is disposed of elsewhere in areas close to cities and rivers. Despite the fact that there are previous works related to the production of activated carbon (AC) from sawdust for dye removal dissolved in water [1, 11], the removal of different chemical structure dyes with low-cost adsorbents is still a major concern [12]. In this framework, the present work aims to use a sawdust-based activated carbon to remove TR, BS4R and BB from aqueous solutions.

2. Materials and Methods

2.1 Activated carbon and characterization

$ZnCl_2$-activated carbon was produced from *Capparis scabrida* sawdust according to the procedure described in previous works [13, 14]. Dried, ground and sieved raw material was mixed with $ZnCl_2$ and carbonized at 600 °C in a nitrogen flux for 2 h. The resulting material was washed with an acid solution and abundant distilled water. Finally, the sample was dried and sieved to reach a particle size of less than 0.25 mm.

The produced AC was characterized to determine its textural, morphological and chemical surface properties. Nitrogen physisorption was performed to determine the textural properties of the produced AC. Nitrogen physisorption measurements at 77 K were performed on a 3Flex sorption apparatus

(Micromeritics, USA). The specific surface area, S_{BET}, was calculated according to the classical Brunauer–Emmett–Teller (BET) theory for p/p_0 = 0.05-0.25. Since the specific surface area, S_{BET}, is not a proper parameter in the case of mesoporous solids containing micropores, the mesopore surface area, S_{meso}, and the micropore volume, V_{micro}, were also evaluated based on the t-plot method using the carbon black STSA , standard isotherm. The net pore volume, V_{net}, was determined from the nitrogen adsorption isotherm at maximum p/p_0 ~0.99. The mesopore-size distribution was evaluated from the adsorption branch of the nitrogen adsorption-desorption isotherm by the Barrett–Joyner–Halenda (BJH) method via the Roberts algorithm, using the carbon black STSA standard isotherm and the assumption of the slit-pore geometry (characterized by the diameter d of the pores). The micropore-size distribution was evaluated from the low-pressure part of the nitrogen adsorption isotherm ($10^{-7} < p/p_0 < 0.05$) by application of the Horvath-Kawazoe solution for the slit-pore geometry of carbonaceous materials geometry (characterized by the width w of the pores) [15].

The surface functional groups in the AC were studied by FTIR analyses (Shimadzu IR-Prestige, Japan).

The morphological characteristics of the macropores in the prepared AC were analyzed using SEM micrographs obtained by a Vega3 Tescan (Czech Republic) SEM.

2.2 Adsorption kinetic tests

Typical batch kinetic experiments were carried out to test the dye adsorption capacity of the produced AC. TR, BS4R and BB were the dyes used at three initial concentrations (10, 30 and 50 mg/l), and the activated carbon doses were 0.5, 1 and 5 g/l. The volume of solutions in the experiments was 250 ml, and 14 aliquots (10 ml) were taken during the 4 h of experimental time. Dyes concentrations were measured using a Merck Pharo 300 spectrophotometer at wavelengths of 428, 508 and 630 nm for TR, BS4R and BB, respectively.

Kinetic data were evaluated by widely used models: pseudo-first [16] and pseudo-second [17]. The nonlinear form of the models was used, and the parameters were calculated using Origin Pro 2018b software.

3. Results and discussion

3.1. Activated carbon characterization

As shown in figure 1a, it is evident that the investigated AC is a microporous-based material, corresponding to the isotherm I type according to the IUPAC classification. Figure 1b indicates that the AC comprises some portion of small mesopores (with pore size < 7 nm) and micropores (inset in figure 1b with pore size ~0.5 nm.

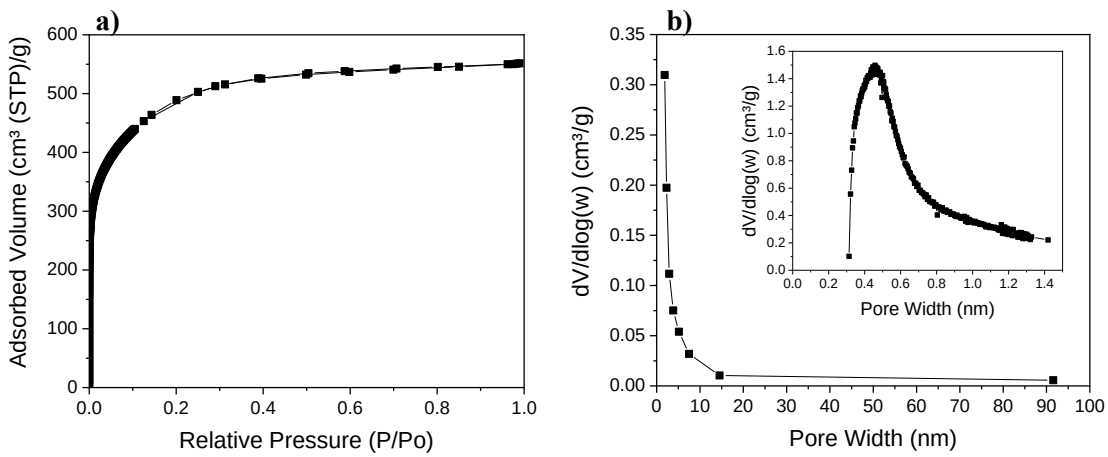

Figure 1. Nitrogen adsorption-desorption isotherm (a) and mesopore-size distributions (b) of the investigated AC. Inset: Micropore-size distribution of the investigated AC.

Capparis scabrida-based AC showed a very high specific surface area close to 1676 m^2/g (table 2) and a high proportion of micropores. The ratio of micropore volume to the net pore volume is ~78%. All determined textural parameters of the investigated AC are summarized in table 2.

Table 2 Textural properties and pH point of zero charge (pH_{PZC}) of the investigated activated carbon.

Material	S_{BET} (m^2/g)	S_{meso} (m^2/g)	V_{micro} (mm^3/g)	V_{net} (mm^3/g)	V_{micro}/V_{net} (%)	pH_{PZC}
Capparis scabrida-based AC	1676	250	667	853	78	3.5

As shown in the micrographs of the AC (see figure 2), it is possible to see the macropores. The shape of the macropores is variable, with predominantly ovoid and irregular shapes.

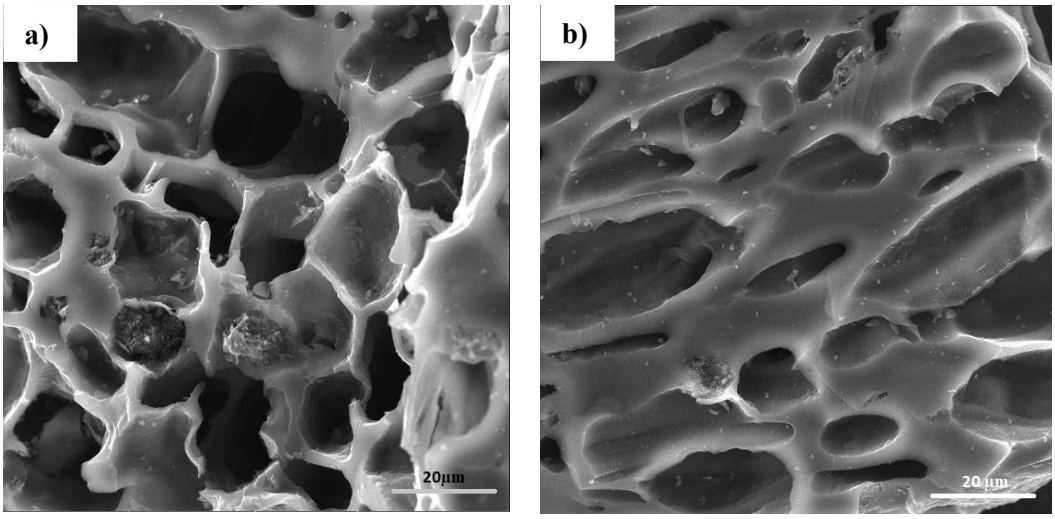

Figure 2. SEM micrographs of the produced AC.

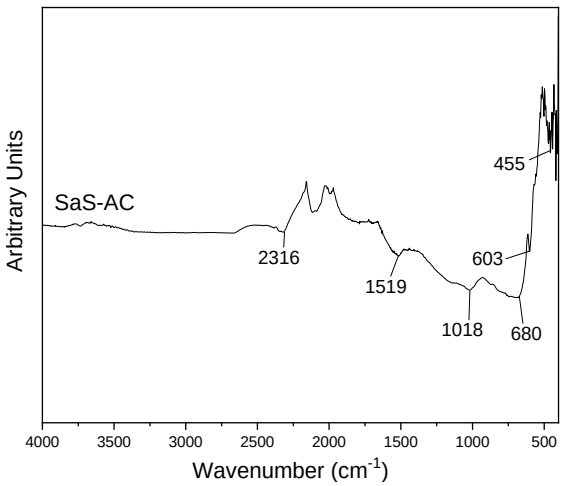

Figure 3. FTIR spectrum of the produced AC.

In the FTIR spectrum of the AC (see figure 3), peaks between 2316 and 455 cm^{-1} are intensive. The peak at 2316 cm^{-1} related to C≡C stretching vibrations in alkyne groups [18] is present. The peak at 1519 cm^{-1} could be assigned to the skeletal C=C stretching vibration in aromatic compounds [19, 20] or C=O in the quinone structure and carboxylate groups [21]; the peak at 1018 cm^{-1} was assigned to the C-O stretching vibration in alcohol, phenol, ether or ester [19, 20, 22] and the peaks at 603 – 680 cm^{-1} were assigned to the O-H bending vibration [20]. Additionally, the peak at approximately 455 cm^{-1} corresponds to the presence of a semiconductor compound. In a previous work, [14] ZnO and ZnS were detected via XRD in AC derived from *Capparis scabrida*. ZnO and ZnS are evolved from the chemical activator ($ZnCl_2$) during the activation process.

3.2. Kinetic Adsorption tests

Adsorption kinetic data for three different dyes, TR, BS4R and BB, are depicted in figure 4. The adsorbent was able to remove the dyes in different intensities; however, establishing an order of AC adsorption efficiency of the dyes could be BS4R>TR>BB. Different authors have studied the adsorption of anionic dyes [8, 23-25], such as the dyes studied in this research, and they coincided in the fact that the best adsorption of TR, BS4R and BB occurs at pH levels less than 3. According to Gautam, Gautam, Banerjee, Lofrano, Sanroman, Chattopadhyaya and Pandey [26], the presence of functional groups such as -OH and C=O over the surface of the adsorbent facilitates the adsorption of anionic dyes at low pH levels. The pH of the initial solution was not measured; however, the usual pH levels of these dye solutions are low, approximately 3.5 [2]. The pH_{PZC} of the adsorbent is 3.5, which means that the pH of the solution is at least similar to pH_{PZC}. This effect supposes that the net charge of the adsorbent is neutral; however, there are positively and negatively charged sites on the surface of the adsorbent. Obviously, protonated dyes can be adsorbed by positively charged sites.

Comparing the kinetic data based on the initial AC load, the equilibrium is quickly reached when the initial AC load is 5 g/l for every initial dye concentration. However, when the initial AC load is 1 and 0.5 g/l, the number of experiments until the equilibrium is reached decreases with the increase in the initial concentration of the dye. This fact is well known, and it is based on the assumption that the higher the amount of adsorbent is, the higher the number of active sites. Another fact that is possible to recognize in the curves is that when the initial concentration of the dye is higher, the equilibrium adsorption value is higher. This effect is based on the affirmation that when the initial adsorbate concentration is higher, the initial driving force is higher as well [2].

In the case of BB adsorption, the process did not reach equilibrium in most cases. The equilibrium is reached when the initial BB concentration is 10 mg/l and the doses of AC are 1 and 5 g/l. This fact could be related to the larger molecular size of the BB molecule compared to that of BS4R and TR, both 1.42 x 0.765 nm [27]. The larger molecular size of the dye could negatively affect the adsorption process since the larger molecular size of the adsorbate does not allow the adsorbate to access small micropores, considering the micropore size ~ 0.5 nm in the investigated AC. Another reason could be related to the pH of the solution during the experiment. The pH of the dye solution during the adsorption process is variable; thus, it could be possible that during BB adsorption, the pH level increases because of the presence of positively charged active site in the BB molecule (N^+), causing a reduction in the adsorption and even fluctuation (increase and decrease) during the time. The presence of positive active sites could cause repulsion with the protonated active sites over the surface of the AC.

The parameters for the dye kinetic adsorptions by AC are shown in table 3. When the initial concentration of dyes is 10 and 30 mg/l, most of the data fit to the pseudo-first and pseudo-second order models (PFO and PSO respectively) with an irregular pattern. In the case of the kinetic data when the initial concentration of dyes is 50 mg/l, the data fit to the both models in the case of TR and BB; however, in the case of BS4R, the data does not fit to the PFO nor PSO when the initial AC load is 0.5 and 1 g/l. When the initial AC load is 5.0 g/l the data fit both models. Despite this tendency, most of the kinetic data present high accordance with more than one kinetic model. This is evidence to postulate that different phenomena (such as mass transfer, chemical bonding, electrostatic forces, etc.) are involved during the dye adsorption process instead of just one.

Analyzing the data that fit well to the pseudo-second order model and considering that the equilibrium was reached, the equilibrium adsorption capacity (q_e) for TR was 55.3 mg/g (when the AC load was 1 g/l and the TR initial concentration was 50 mg/l); for BS4R, 72.1 mg/g (when the AC load was 1 g/l and the TR initial concentration was 50 mg/l); and for BB, 14.1 mg/g (when the AC load was 1 g/l and the TR initial concentration was 10 mg/l) as the maximum values.

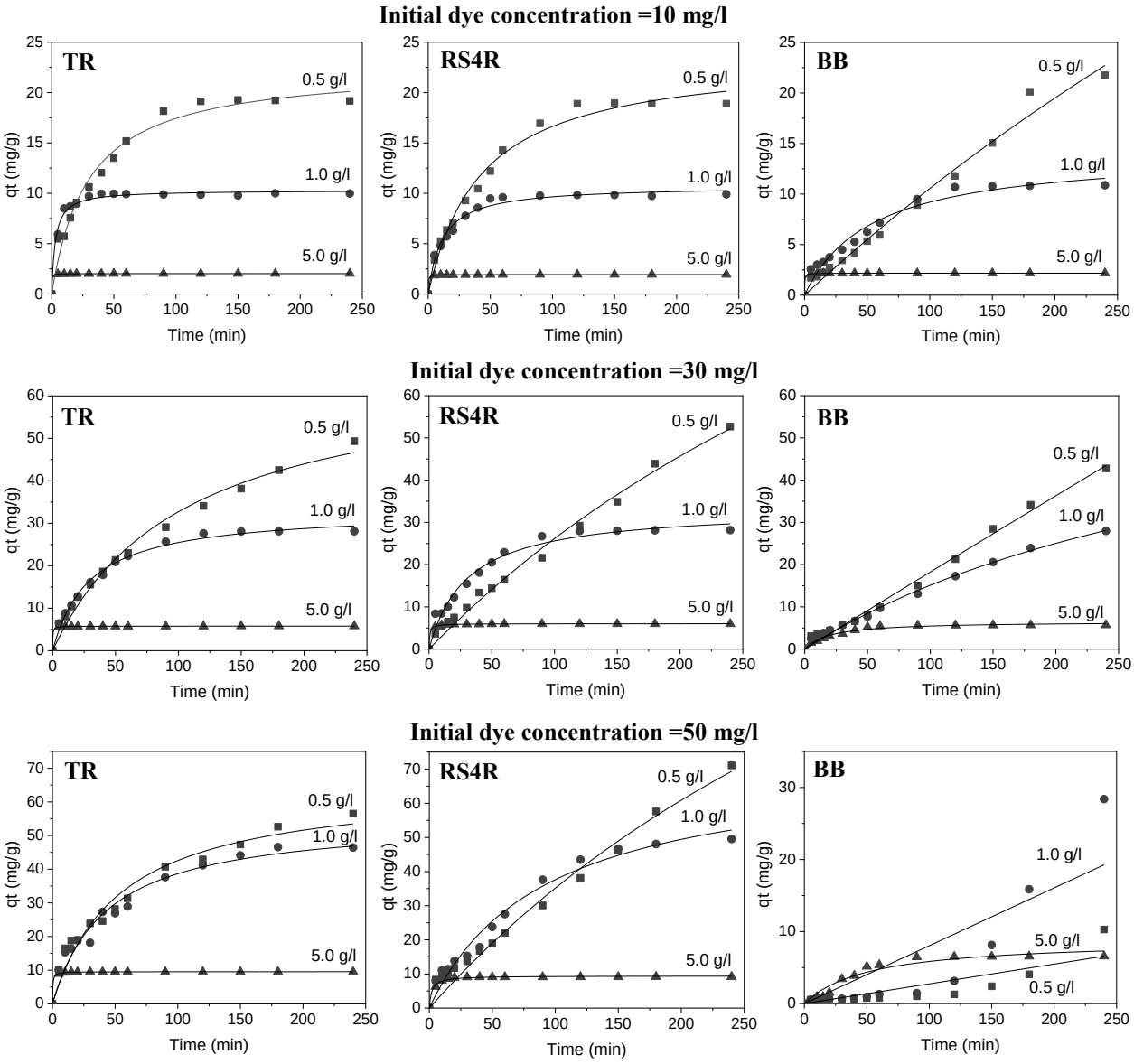

Figure 4. TR, BS4R and BB adsorption kinetic data using different initial concentrations of the dye (10, 30 and 50 mg/l) and different initial activated carbon doses (0.5, 1 and 5 mg/l).

Table 3. Parameters of dye adsorption data by AC based on sawdust biomass.

Parameter	10 mg/l-0.5 g/l	10 mg/l-1.0 g/l	10 mg/l-5.0 g/l	30 mg/l-0.5 g/l	30 mg/l-1.0 g/l	30 mg/l-5.0 g/l	50 mg/l-0.5 g/l	50 mg/l-1.0 g/l	50 mg/l-5.0 g/l
TR									
Pseudo-first order									
q_e (mg/g)	19.22	9.82	2.01	49.41	27.98	5.74	52.80	45.57	9.48
k_1(min^{-1})	0.028	0.178	0.769	0.011	0.029	0.691	0.017	0.021	0.566
X^2	1.179	0.063	1.31x10^{-4}	5.576	1.187	0.001	17.918	11.87	0.002
R^2	0.97	0.99	0.99	0.98	0.99	0.99	0.94	0.95	0.99
Pseudo-second order									
q_e (mg/g)	22.56	10.30	2.03	67.09	32.99	5.78	65.46	55.26	9.56
k_2 (g/mg min)	0.001	0.033	3.533	1.416x10^{-4}	0.001	0.965	2.83x10^{-4}	4.212x10^{-4}	0.343
X^2	0.856	0.093	3.79x10^{-5}	3.451	0.744	0.000	11.098	7.835	0.002
R^2	0.98	0.99	1.00	0.99	0.99	1.00	0.96	0.97	1.00
BS4R									
Pseudo-first order									
Parameter	**10 mg/l-0.5 g/l**	**10 mg/l-1.0 g/l**	**10 mg/l-5.0 g/l**	**30 mg/l-0.5 g/l**	**30 mg/l-1.0 g/l**	**30 mg/l-5.0 g/l**	**50 mg/l-0.5 g/l**	**50 mg/l-1.0 g/l**	**50 mg/l-5.0 g/l**
q_e (mg/g)	19.36	9.76	1.93	105.30	28.30	5.93	136.31	53.17	9.10
k_1(min^{-1})	0.023	0.061	0.684	0.003	0.029	0.450	0.003	0.013	0.229
X^2	0.589	0.210	2.49 x10^{-4}	2.931	2.254	0.004	10.859	6.422	0.005
R^2	0.99	0.98	1.00	0.99	0.98	1.00	0.98	0.98	1.00
Pseudo-second order									
q_e (mg/g)	23.67	10.74	1.94	179.58	33.39	6.02	227.85	72.04	9.42
k_2 (g/mg min)	9.96 x10^{-4}	0.008	2.431	9.49 x10^{-6}	9.84 x10^{-4}	0.281	8.0 x10^{-6}	1.51 x10^{-4}	0.055
X^2	0.674	0.175	6.98x10^{-5}	2.824	2.114	0.001	10.535	7.013	0.056
R^2	0.99	0.98	1.00	0.99	0.98	1.00	0.98	0.98	0.99
BB									
Pseudo-first order									
q_e (mg/g)	69.24	11.28	2.17	4222.99	44.04	5.73	38182.84	118469.70	6.95
k_1(min^{-1})	0.002	0.019	0.682	4.31 x10^{-5}	0.004	0.04	7.18 x10^{-7}	6.78 x10^{-7}	0.021
X^2	0.816	0.468	5.28x10^{-5}	1.493	0.664	0.047	2.108	17.336	0.247
R^2	0.98	0.97	1.00	0.99	0.99	0.99	0.73	0.76	0.97
Pseudo-second order									
q_e (mg/g)	129.41	14.13	2.17	3221.76	72.53	6.54	8480.01	25859.80	8.88
k_2 (g/mg min)	6.85 x10^{-6}	0.001	2.636	1.76 x10^{-8}	3.63 x10^{-5}	0.007	3.816 x10^{-10}	1.201 x10^{-10}	0.002
X^2	0.820	0.474	2.91 x10^{-5}	1.500	0.640	0.098	2.109	17.347	0.407
R^2	0.98	0.97	1.00	0.99	0.99	0.97	0.73	0.76	0.95

q_t = amount of adsorbate adsorbed per mass of adsorbent at time t (mg/g); q_e =amount of adsorbate adsorbed per mass of adsorbent at equilibrium (mg/g); k_1 = rate constant of the PFO equation (1/min); k_2 = rate constant of the PSO equation (g/mg x min); X^2 is chi square and R^2 is the coefficient of determination

4. Conclusions

The adsorbent (activated carbon) prepared by the chemical activation of *Capparis scabrida* residual biomass was able to remove tartrazine (TR), brilliant scarlet 4R (BS4R) and brilliant blue (BB) at different intensities; however, the order of adsorption ability was as follows: BS4R>TR>BB. Most of the kinetic data fit best to the pseudo-second order model; however, a high accordance with other models reveals that there is more than one phenomenon to explain the adsorption process. Analyzing the data that fit well to the pseudo-second order model and considering that the equilibrium was reached, the equilibrium adsorption capacity (q_e) for TR was 55.3 mg/g (when the AC load was 1 g/l and the TR initial concentration was 50 mg/l); for BS4R, 72.1 mg/g (when the AC load was 1 g/l and the TR initial concentration was 50 mg/l); and for BB, 14.1 mg/g (when the AC load was 1 g/l and the TR initial concentration was 10 mg/l) as the maximum values. AC based on *Capparis scabrida* residual biomass is a promising material for use in the purification of water polluted by anionic azo dyes.

Acknowledgments

The National University of Tumbes (CANON project – R.N° 0169-2017/UNT-R) and the Peruvian National Council for Science and Technology (CONCYTEC) (Contract N° 024-2016-FONDECYT) are gratefully acknowledged for their support.

References

[1] Aguayo-Villarreal I A, Hernández-Montoya V, Ramírez-López E M, Bonilla-Petriciolet A and Montes-Morán M A 2016 Effect of surface chemistry of carbons from pine sawdust for the adsorption of acid, basic and reactive dyes and their bioregeneration using Pseudomona putida *Ecological Engineering* **95** 112-8

[2] Duygu Ozsoy H and van Leeuwen J 2010 Removal of color from fruit candy waste by activated carbon adsorption *Journal of Food Engineering* **101** 106-12

[3] Ahmad A, Mohd-Setapar S H, Chuong C S, Khatoon A, Wani W A, Kumar R and Rafatullah M 2015 Recent advances in new generation dye removal technologies: novel search for approaches to reprocess wastewater *RSC Advances* **5** 30801-18

[4] A Kassem M and El-Sayed G O 2014 Adsorption of Tartrazine on Medical Activated Charcoal Tablets under Controlled Conditions *Journal of Environmental Analytical Chemistry* **01**

[5] Lucova M, Hojerova J, Pazourekova S and Klimova Z 2013 Absorption of dyes Brilliant Blue and Patent Blue through intact skin, shaven skin and lingual mucosa from daily life products *Food Chem Toxicol* **52** 19-27

[6] Yamjala K, Nainar M S and Ramisetti N R 2016 Methods for the analysis of azo dyes employed in food industry--A review *Food Chem* **192** 813-24

[7] Habila M A, Alothman Z A, Ali R, Ghafar A A and Hassouna M S E-D 2014 Removal of Tartrazine Dye onto Mixed-Waste Activated Carbon: Kinetic and Thermodynamic Studies *CLEAN - Soil, Air, Water* **42** 1824-31

[8] Tikhomirova T I, Ramazanova G R and Apyari V V 2014 Sorption of Ponceau 4R anionic dye from aqueous solutions on aluminum oxide and polyurethane foam *Russian Journal of Physical Chemistry A* **88** 2192-6

[9] Tikhomirova T I, Ramazanova G R and Apyari V V 2018 Effect of nature and structure of synthetic anionic food dyes on their sorption onto different sorbents: Peculiarities an prospects *Microchemical Journal* **143** 305-11

[10] Gosetti F, Gianotti V, Angioi S, Polati S, Marengo E and Gennaro M C 2004 Oxidative degradation of food dye E133 Brilliant Blue FCF *Journal of Chromatography A* **1054** 379-87

[11] Doltabadi M, Alidadi H and Davoudi M 2016 Comparative study of cationic and anionic dye removal from aqueous solutions using sawdust-based adsorbent *Environmental Progress & Sustainable Energy* **35** 1078-90

[12] Tezcan Un U and Ates F 2018 Low-cost adsorbent prepared from poplar sawdust for removal of disperse orange 30 dye from aqueous solutions *International Journal of Environmental Science and Technology*

[13] Cruz G J F, Matějová L, Pirilä M, Ainassaari K, Canepa C A, Solis J, Cruz J F, Šolcová O and Keiski R L 2015 A Comparative Study on Activated Carbons Derived from a Broad Range of Agro-industrial Wastes in Removal of Large-Molecular-Size Organic Pollutants in Aqueous Phase *Water, Air, & Soil Pollution* **226**

[14] Cruz J, Cruz G, Ainassaari K, Gómez M, Solís J and Keiski R 2018 Microporous activation carbon made of sawdust from two forestry species for adsorption of methylene blue and heavy metals in aqueous system - Case of real pulluted water *Revista Mexicana de Ingeniería Química* **17** 847-61

[15] Cruz G J F, Kuboňová L, Aguirre D Y, Matějová L, Peikertová P, Troppová I, Cegmed E Wach A, Kustrowski P, Gomez M M and Obalová L 2017 Activated Carbons Prepared from a Broad Range of Residual Agricultural Biomasses Tested for Xylene Abatement in the Gas Phase *ACS Sustainable Chemistry & Engineering* **5** 2368-74

[16] Lagergren S 1898 About the theory of so-called adsorption of soluble substances *K. Sven. Vetens. Handl.* **24** 1-39

[17] Blanchard G, Maunaye M and Martin G 1984 Removal of heavy metals from waters by means of natural zeolites *Water research* **18** 1501-7

[18] Saka C 2012 BET, TG–DTG, FT-IR, SEM, iodine number analysis and preparation of activated carbon from acorn shell by chemical activation with ZnCl2 *Journal of Analytical and Applied Pyrolysis* **95** 21-4
[19] Liou T-H 2010 Development of mesoporous structure and high adsorption capacity of biomass-based activated carbon by phosphoric acid and zinc chloride activation *Chemical Engineering Journal* **158** 129-42
[20] Sahu J, Acharya J and Meikap B 2010 Optimization of production conditions for activated carbons from Tamarind wood by zinc chloride using response surface methodology *Bioresource technology* **101** 1974-82
[21] Oliveira L C, Pereira E, Guimaraes I R, Vallone A, Pereira M, Mesquita J P and Sapag K 2009 Preparation of activated carbons from coffee husks utilizing $FeCl_3$ and $ZnCl_2$ as activating agents *Journal of Hazardous Materials* **165** 87-94
[22] Angin D 2014 Production and characterization of activated carbon from sour cherry stones by zinc chloride *Fuel* **115** 804-11
[23] Gautam R K, Gautam P K, Banerjee S, Rawat V, Soni S, Sharma S K and Chattopadhyaya M C 2015 Removal of tartrazine by activated carbon biosorbents of Lantana camara: Kinetics, equilibrium modeling and spectroscopic analysis *Journal of Environmental Chemical Engineering* **3** 79-88
[24] Gupta V K, Mittal A, Krishnan L and Mittal J 2006 Adsorption treatment and recovery of the hazardous dye, Brilliant Blue FCF, over bottom ash and de-oiled soya *J Colloid Interface Sci* **293** 16-26
[25] Mittal A 2006 Use of hen feathers as potential adsorbent for the removal of a hazardous dye, Brilliant Blue FCF, from wastewater *J Hazard Mater* **128** 233-9
[26] Gautam P K, Gautam R K, Banerjee S, Lofrano G, Sanroman M A, Chattopadhyaya M C and Pandey J D 2015 Preparation of activated carbon from Alligator weed (Alternenthera philoxeroids) and its application for tartrazine removal: Isotherm, kinetics and spectroscopic analysis *Journal of Environmental Chemical Engineering* **3** 2560-8
[27] Vargas A M M, Cazetta A L, Martins A C, Moraes J C G, Garcia E E, Gauze G F, Costa W F and Almeida V C 2012 Kinetic and equilibrium studies: Adsorption of food dyes Acid Yellow 6, Acid Yellow 23, and Acid Red 18 on activated carbon from flamboyant pods *Chemical Engineering Journal* **181-182** 243-50